International Journal of Heat and Technology
Vol. 44, No. 3, June, 2026, pp. 1215-1226
Journal homepage: http://iieta.org/journals/ijht

Experimental Investigation of Thermodynamic Irreversibility and Exergy Destruction in a Diesel Engine Fueled with Waste Cooking Oil Biodiesel Blends

Karrar S. Hasan[1*], Hyder H. Balla[2]

[1] Department of Mechanical Engineering Techniques of Power, Technical College Najaf, Al-Furat Al-Awsat Technical University, Najaf 54001, Iraq
[2] Department of Aeronautical Technical, Najaf Technical Institute, Al-Furat Al-Awsat Technical University, Najaf 54001, Iraq

Corresponding Author Email: eng.karrarsalah@atu.edu.iq

https://doi.org/10.18280/ijht.440327

Received: 15 March 2026
Revised: 30 May 2026
Accepted: 9 June 2026
Available online: 30 June 2026

Keywords:
alternative fuels, biodiesel blends, compression ignition engine, exergy analysis, exergy destruction, experimental uncertainty, thermodynamic irreversibility, Waste Cooking Oil biodiesel

ABSTRACT

This study experimentally investigates the thermodynamic and exergy behavior of waste cooking oil (WCO) biodiesel blends (B10–B50) in an unmodified single-cylinder diesel engine operating at 1500 rpm under loads from 25% to 100%. First-law performance parameters, including brake specific fuel consumption (BSFC), brake thermal efficiency (BTE), exhaust gas temperature (EGT), and air-fuel ratio (AFR), together with exergy efficiency (η_{ex}) and exergy destruction, were evaluated. Experimental uncertainty was determined using the root-sum-square (RSS) method. Biodiesel blends at increased load levels raised EGT by approximately 6.8% and BSFC by approximately 10.7% due to differences in heating value and viscosity. Under full-load conditions, the AFR and volumetric efficiency of biodiesel blends were approximately 8.3% and 3.1% lower, respectively, than those of pure diesel (D100). η_{ex} increased with engine load, reaching 21.34% for pure diesel at full load. Higher exergy destruction in B50 (18.52 kW) compared to D100 (15.13 kW) indicates greater thermodynamic irreversibility within the adopted exergy-based evaluation framework as the blending ratio of biodiesel is increased. The uncertainty in the derived thermodynamic parameters did not exceed 2–3%, indicating acceptable experimental reliability. The results indicate that low and medium biodiesel blends (B10-B20) can be used in a conventional diesel engine without modification while maintaining acceptable thermodynamic performance.

1. INTRODUCTION

Waste cooking oil (WCO) biodiesel is considered a suitable alternative to petroleum diesel in compression-ignition engines. It is renewable and naturally biodegradable. In addition, it can be used in conventional diesel engines with little or no mechanical modification [1, 2]. Fuel shortages and harmful exhaust emissions have increased interest in cleaner and more sustainable fuels [3]. In addition to saving costs, recycling WCO to make biodiesel also contributes to a reduction in environmental pollution and better energy recovery. There are various fuel properties that influence the combustion behavior of biodiesel blends, such as density, viscosity, oxygen content and heating value. These properties affect the spray formation, ignition delay, combustion stability and heat release within the cylinder [4, 5]. Biodiesel blends are generally associated with lower carbon monoxide and hydrocarbon emissions. However, the higher the biodiesel ratio, the more fuel that will be consumed, and under certain operating conditions, the combustion temperature will also increase. Thus, it is still necessary to identify appropriate blending ratios for ensuring the desired thermodynamic performance and stable engine operation without changing the engine system.

Exergy analysis has become an effective method for evaluating the thermodynamic performance of biodiesel-fueled diesel engines because it provides deeper insight into energy quality and system irreversibility [6, 7]. Exergy analysis can also identify the thermodynamic losses that occur in combustion and heat transfer systems and quantify the loss of useful energy in them, unlike conventional energy analysis. The previous studies also revealed that an integrated energy and exergy analysis offers a comprehensive insight into the behavior of a diesel engine under practical operating conditions [8]. In addition, biodiesel–diesel blends were found to improve thermodynamic behavior and reduce exergy destruction under suitable operating conditions [9, 10]. The effect of biodiesel blends on engine performance and emissions has been the subject of several studies. In general, biodiesel fuels contribute to cleaner combustion because of their oxygenated structure [11, 12]. Experimental studies reported improvements in combustion behavior and thermal performance at medium engine loads when suitable biodiesel blending ratios were used [13]. Other studies showed that increasing the biodiesel ratio may increase BSFC and combustion temperature, particularly at high engine loads [14, 15]. Similar observations were reported by Hossain et al. [8], Abed et al. [16], Sayyed et al. [17], and Mathew et al. [18], where biodiesel blends reduced some harmful emissions but also affected fuel consumption and combustion characteristics under different operating conditions. Recent investigations further highlighted the importance of combining energy, exergy, and sustainability assessments for biodiesel-powered diesel engines [19, 20].

Despite the large number of studies on biodiesel utilization in compression-ignition engines, most previous investigations focused mainly on first-law performance indicators, BTE and BSFC. These approaches do not fully explain thermodynamic losses and internal irreversibility within the engine system. In addition, many previous studies investigated high biodiesel blending ratios or required engine modifications to achieve lower emissions [21-23]. Limited attention has been given to medium-range biodiesel blends (B10–B50) operating in unmodified diesel engines under practical conditions. Furthermore, the combined assessment of thermodynamic performance, exergy behavior, and experimental uncertainty remains insufficiently explored [24, 25]. Therefore, the exergy approach to the energy degradation and irreversibility of the useful energy is more informative, and if it is not used, a comprehensive interpretation of the thermodynamics of the diesel engine is limited [26, 27]. In diesel engines, exergy analysis is a second law-based approach to the determination of the magnitude and distribution of thermodynamic losses and has proven to be a useful tool for assessing the performance under varying operating conditions [28]. The present study integrates the methods of energy analysis, exergy analysis, and uncertainty quantification for WCO biodiesel blends in an unmodified diesel engine, whereas most of the previous studies have concentrated on the first-law approach. The study examines the biodiesel blends from B10 to B50 in practical operating conditions of the engine with the aim of evaluating the thermodynamic behavior and practical application of the biodiesel blends without the engine's mechanical modification.

2. MATERIALS AND EXPERIMENTAL METHODS

2.1 Preparation of waste cooking oil biodiesel blend

This study involved the laboratory preparation of biodiesel from WCO through a base-catalysed transesterification process, as depicted in Figure 1. The procedure commenced with the refinement of the WCO. One litre of WCO was passed through a fine membrane filter to remove impurities and solid particulates. To prevent saponification during the transesterification process, the filtered oil was heated to 65 °C for 30 min and subsequently dried to remove any residual moisture [29].

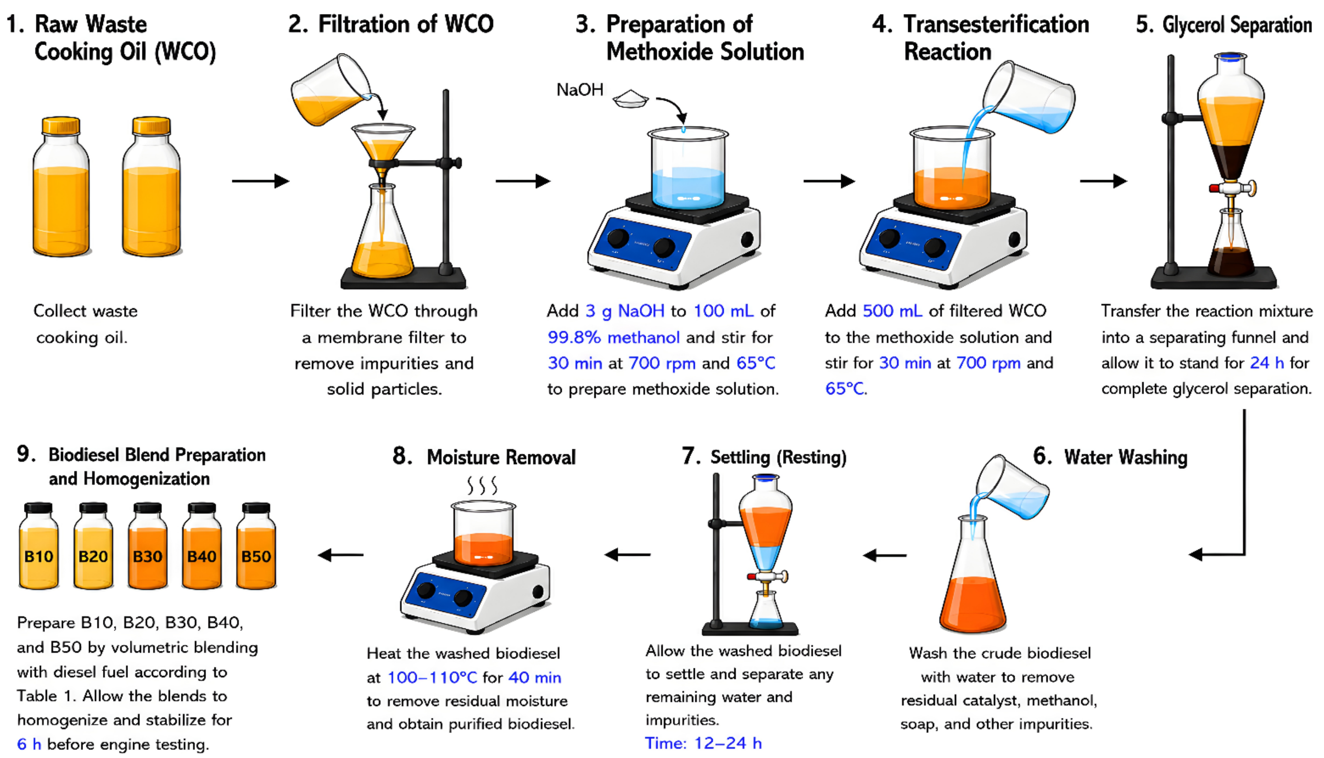

Figure 1. Schematic illustration of the waste cooking oil (WCO) biodiesel production process and biodiesel–diesel blend preparation

Table 1. Detailed volumetric composition of experimental fuel blends (per 1000 mL)

Fuel Designation	Base Diesel (mL)	Waste Cooking Oil (WCO) Biodiesel (mL)	Total Volume (mL)
D100	1000	0	1000
B10	900	100	1000
B20	800	200	1000
B30	700	300	1000
B40	600	400	1000
B50	500	500	1000

Table 2. Physicochemical properties of experimental fuel blends

Fuel / Blend	Biodiesel (vol.%)	Density @20 °C (kg/m³)	Calorific value (kJ/kg)	Flash point (°C)	Pour point (°C)	Cetane Index (–)	Kinematic viscosity @40 °C (mm²/s)
D100	0	830	43000	68	−16	53.4	2.70
B10	10	836	42650	78	−14	53.7	2.92
B20	20	841	42300	92	−12	54.1	3.15
B30	30	846	41950	108	−10	54.6	3.39
B40	40	852	41600	128	−8	55.1	3.66
B50	50	858	41250	150	−6	55.9	3.98
B100	100	885	39250	181	−3	56.7	4.87

Note: Fuel properties were determined according to ASTM D4052 (density), ASTM D240 (calorific value), ASTM D93 (flash point), ASTM D97 (pour point), and ASTM D445 (kinematic viscosity).

The first treatment was followed by transesterification with methanol and sodium hydroxide (NaOH) as alcohol and base catalyst, respectively. 100 mL of 99.8% methanol with 3 g of NaOH (molar ratio of methanol: oil of 5:1) was prepared for every 500 mL of filtered WCO. The methanol / NaOH solution was stirred for 30 min at 65 °C with a stirring rate of 700 rpm and then mixed with WCO. The reaction mixture was then kept under continuous magnetic stirring (700 rpm) and heating (65 °C) for another 30 min to confirm the complete transesterification process. Upon completion of the reaction, the mixture was transferred into a separating funnel and allowed to stand for 24 h. Gravity-induced phase separation produced a lower glycerol layer and an upper crude biodiesel layer. The crude biodiesel was subsequently washed with water to remove residual catalyst, methanol, soap, and other impurities. The washed biodiesel was then heated at 100–110 °C for 40 min to remove residual moisture and obtain purified biodiesel suitable for engine testing [30]. The five biodiesel mixtures were ultimately prepared as illustrated in Table 1. Before engine testing, all biodiesel–diesel blends (B10–B50) were allowed to homogenize and stabilize for 6 h to ensure uniform fuel properties throughout the experiments.

The prepared biodiesel blends were subjected to various physicochemical property analysis in the laboratories of the Aeronautical Technical Department of Najaf Technical Institute by employing the respective ASTM standard methods as listed in Table 2. The measured values were then compared to the requirements of ASTM D6751 and EN 14214. The kinematic viscosity remained within the acceptable range reported in previous studies (1.9–6.0 mm²/s), while the remaining fuel properties also satisfied the specified standards [31, 32]. Figure 2 shows the biodiesel blends prepared for testing, and Table 2 summarizes their measured physicochemical properties.

2.2 Engine configuration and test rig

All experiments were conducted in the Combustion Laboratory of the Aeronautical Technical Department at Najaf Technical Institute, Al-Furat Al-Awsat Technical University. An Altaj SA-100 diesel engine was used, as detailed in Figure 3; Figure 4 shows its schematic. The engine was a single-cylinder, four-stroke, air-cooled, direct-injected engine. A control panel that included gauges was a must in order to make the experiments possible. This panel featured switches for the fuel loads, a voltmeter/ammeter, a tachometer and a graduated cylinder to measure fuel consumption. Also installed in this system were an air filter, a calibrated orifice meter, and a digital, differential manometer for measuring the air-flow rate into the system. The engine's technical specifications are shown in Table 3.

2.2.1 Measurement instruments and data acquisition

During the experiments, a number of measuring instruments were used, and their characteristics and technical specifications are shown in Table 4.

Table 3. Specifications of the experimental diesel engine

Specification	Value
Model	SA-100
Type	Single Cylinder, 4-Stroke, Air-Cooled
Combustion System	Direct Injection (DI)
Bore × Stroke	102 × 110 mm
Displacement Volume	899 cc
Rated Output	7.35 kW (10 hp) @ 1500 rpm
Compression Ratio	17:1
Lubrication	Force feed and splash lubrication
Net Weight	180 kg

Figure 2. Prepared waste cooking oil (WCO) biodiesel–diesel blends (B10–B50) used in the experimental investigation

Figure 3. Photograph of the experimental diesel engine test rig

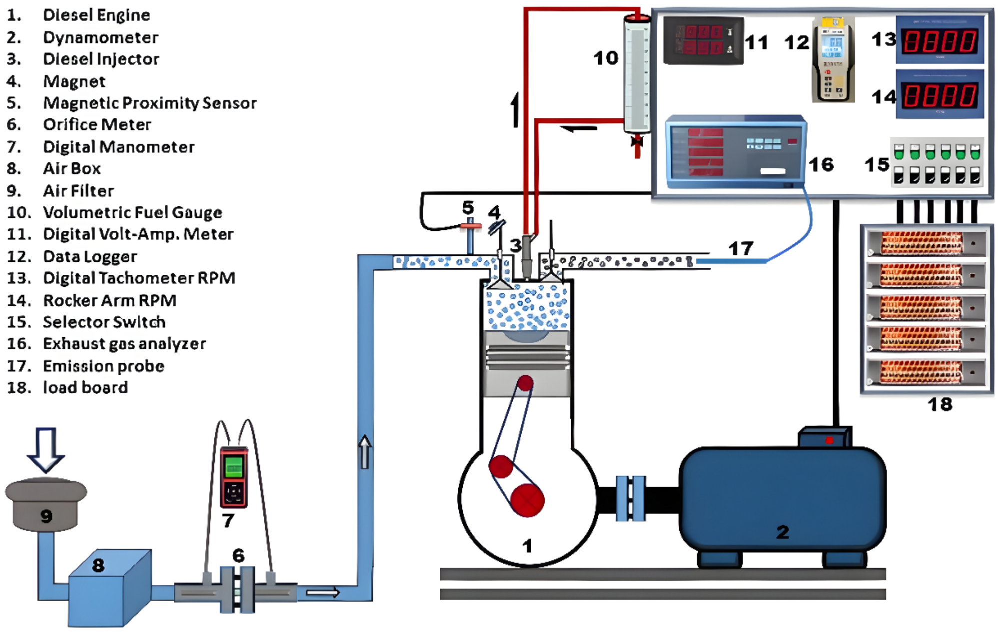

Figure 4. Schematic diagram of the experimental diesel engine test rig

Table 4. Technical characteristics of auxiliary measurement instrumentation

Specification / Model	Parameter Measured	Instrument
Model: EHDIS, Range: ±2.999 psi	Intake Manifold Pressure	Digital Manometer
Digital sensor	Engine Speed	Tachometer
Calibrated volumetric burette (pipette)	Fuel Consumption	Fuel Gauge
K-type thermocouples	EGT, Fuel, Air Temp	Temperature Sensors
Model: HT-9815	Records data from sensors (e.g., Temp.)	Data Logger

The intake air flow rate was measured using a calibrated orifice meter connected to a digital differential manometer. The orifice geometry is illustrated in Figure 5 (D = 40 mm, d = 20 mm, β = 0.5, Cd = 0.6). The measured differential pressure was subsequently used to determine the intake air mass flow rate.

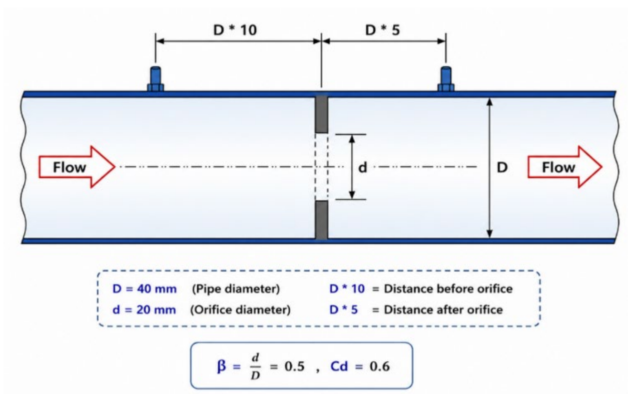

Figure 5. Schematic diagram of the orifice meter used to measure the intake air-flow rate

2.3 Experimental procedure

All experiments were conducted with consistent operating conditions using a single-cylinder diesel engine to ensure accuracy, repeatability, and feasibility of the experiments. The engine speed and compression ratio were maintained at 1500 rpm and 17:1, respectively, during the test. The performance and emission data were then taken with the engine at 0%, 25%, 50%, 75%, and 100% of its maximum capacity. The reference fuel and baseline fuel were diesel fuel (D100), and it was blended with WCO biodiesel at volumetric concentrations from B10 to B50 to be compared. The methodology was replicated with different fuel formulations to enhance the accuracy of the test and increase confidence in the data obtained. The study included analyses of fuel consumption rates, braking power, exhaust gas temperature (EGT), and pollutant concentrations. Specific equations were used in Microsoft Excel to perform accurate calculations, facilitating the assessment of BSFC and BTE. The gathered data were utilised to conduct both first-law and second-law thermodynamic analyses. This approach facilitated the utilization of an unaltered mechanical engine, attaining a balance between emission reduction and thermodynamic efficiency.

3. THERMODYNAMIC AND UNCERTAINTY ANALYSIS

3.1 Energy-based performance analysis

3.1.1 Electrical power output

The engine load was represented by the electrical power output of the coupled single-phase synchronous generator, which was calculated from the measured voltage and current according to Eq. (1). Since the generator operated at a unity power factor (cosφ = 1.0), the electrical power output was determined directly from the measured electrical parameters.

$$P = \frac{V.I}{1000} \quad (1)$$

where, P = electrical power output (kW), V is the measured voltage (V), and I is the measured current (A).

3.1.2 Brake Specific Fuel Consumption

In the present study, BSFC was calculated using the measured electrical power output of the coupled synchronous generator, which was considered as the useful engine output:

$$BSFC = \frac{m_f^{\cdot}}{P_{elec}} \tag{2}$$

In g/kWh, the following relation was used:

$$BSFC(g/kWh) = \frac{m_f^{\cdot}\left(\frac{kg}{s}\right).3600}{P_{elec}} \tag{3}$$

where, $m_f^{\cdot}$ is the fuel mass flow rate, and P_{elec} is the measured electrical power output.

3.1.3 Brake Thermal Efficiency

The BTE expresses the ratio of useful electrical power output to the fuel energy input.

$$BTE = \frac{P_{elec}}{LHV.m_f^{\cdot}} \tag{4}$$

where, LHV = The lower heating value of the fuel blends (kJ/kg).

3.1.4 Air-Fuel ratio

The intake air mass flow rate was experimentally measured using a calibrated orifice meter installed in the engine intake system and connected to a digital differential manometer. The air mass flow rate was determined from the measured pressure drop across the orifice according to:

$$m_a^{\cdot} = C_d A_0 \sqrt{2\rho_a \Delta P} \tag{5}$$

where, C_d is the discharge coefficient, A_0 is the orifice area, ρ_a is the ambient air density, and ΔP is the measured differential pressure. The AFR was then calculated as:

$$AFR = \frac{m_a^{\cdot}}{m_f^{\cdot}} \tag{6}$$

3.1.5 Volumetric efficiency

The measured intake air mass flow rate was used to determine the volumetric efficiency (η_v) of the four-stroke diesel engine based on the following:

$$\eta_v = \frac{m_a^{\cdot}}{\rho_a V_d N/2} \tag{7}$$

where, V_d is the engine displacement volume, and N is the engine speed. The factor of 2 in the denominator accounts for the four-stroke operating cycle, where one intake event occurs every two crankshaft revolutions.

3.2 Exergy-based thermodynamic analysis

Exergy analysis accounts for energy quality and system irreversibility during combustion and heat transfer processes.

3.2.1 Reference state and assumptions

To perform the second-law analysis (exergy analysis), the reference environment was assumed at T_o= 298 K and P_o = 1 atm. Exergy is defined relative to the reference environment, since no useful work can be extracted once equilibrium is reached. A chemical exergy factor (X = 1.04) was adopted for the fuel blends to account for the difference between chemical exergy and lower heating value. The specific heat capacity of exhaust gases was assumed constant (Cp = 1.1 kJ/kg·K), which is a common approximation for diesel engine exhaust analysis.

3.2.2 Fuel chemical exergy

The fuel exergy rate, $\dot{E}x_{fuel}$, represents the available work potential from the fuel during complete combustion relative to the environment. It was calculated as:

$$\dot{E}x_{fuel} = m_f^{\cdot}.LHV.X \tag{8}$$

where, $m_f^{\cdot}$ is the fuel mass flow rate (kg/s), and LHV is the lower heating value (kJ/kg). The chemical exergy factor X accounts for deviations between chemical exergy and heating value.

3.2.3 Electrical power exergy rate

The useful electrical power output of the engine–generator system was determined from the measured voltage and current. The electrical exergy rate was assumed equal to the electrical power output because electrical energy can be completely converted into useful work under ideal conditions.

$$\dot{E}x_{elec} = P_{elec} \tag{9}$$

3.2.4 Physical exergy of exhaust gases

The physical exergy of exhaust gases was estimated based on the temperature difference between exhaust gases and the reference environment, and it was estimated as follows:

$$\dot{E}x_{exh} = \dot{m}_{ex}\,.Cp\left[(T_{exh} - T_o) - T_o\,ln\left(\frac{T_{exh}}{T_o}\right)\right] \tag{10}$$

where, the exhaust mass flow rate ($\dot{m}_{ex}$) is the sum of fuel ($m_f^{\cdot}$) and air ($m_a^{\cdot}$) mass flow rates:

$$\dot{m}_{ex} \approx m_f^{\cdot} + m_a^{\cdot} \tag{11}$$

$$\dot{m}_a = AFR.m_f^{\cdot} \tag{12}$$

Exhaust exergy indicates the recoverable work potential available for waste heat recovery systems (WHRs) [24].

3.2.5 Exergy destruction

Exergy destruction ($\dot{E}x_{dest}$) represents the portion of fuel exergy irreversibly lost due to internal entropy generation within the engine. It was determined using the steady-state exergy balance:

$$\dot{E}x_{dest} = \dot{E}x_{fuel} - (\dot{E}x_{elec} + \dot{E}x_{exh}) \tag{13}$$

where, $\dot{E}x_{elec}$ is the useful electrical power output exergy and $\dot{E}x_{exh}$ is the physical exergy associated with the exhaust gases. A higher exergy destruction rate indicates greater thermodynamic irreversibility and reduced system effectiveness [33].

A simplified exergy balance was used to evaluate the thermodynamic performance of the diesel engine in the present study. The exergy destruction was calculated as the difference between the exergy input of the fuel and the useful electrical power output, and the physical exergy of exhaust gases. The cooling loss, lubrication loss, unburned fuel loss and the chemical exergy of the exhaust gas have not been calculated explicitly in the exergy balance but have been included in the calculated exergy destruction term. The simplified method was also followed to ensure the same operating conditions for all blends of biodiesel to be evaluated similarly.

3.2.6 Exergetic efficiency

Exergetic efficiency (η_{ex}) is the ratio of the useful ratio of the useful electrical power output to the fuel exergy input. It was defined as:

$$\eta_{ex}(\%) = \left(\frac{\dot{E}x_{elec}}{\dot{E}x_{fuel}}\right).100 \quad (14)$$

Unlike BTE, η_{ex} accounts for energy quality and irreversibility. Therefore, it provides a more realistic indicator of thermodynamic performance. Higher η_{ex} reflects improved utilisation of the fuel's work potential and reduced internal losses [25].

3.3 Experimental uncertainty analysis

3.3.1 Instrument accuracy and measurement uncertainty

Instrument accuracies/resolutions were taken from the experimental setup specifications and used to quantify measurement uncertainty and propagate it to derived performance and exergy metrics. The specifications and measurement accuracies of the instruments used in this study are summarized in Table 5.

3.3.2 Root-Sum-Square-based uncertainty propagation

Uncertainty propagation was performed using the root-sum-square (RSS) method. For a derived quantity y = f(x_1, x_2, …, x_n), the combined relative uncertainty is:

$$\frac{U_y}{y} = \sqrt{\sum_{i=1}^{n}(\frac{\partial \ln y}{\partial \ln x_i})^2(\frac{U_{xi}}{xi})^2} \quad (15)$$

where, $\frac{U_y}{y}$ is the relative uncertainty of the derived parameter y, $\frac{U_{xi}}{xi}$ is the uncertainty associated with the measured variable xi.

Table 5. Technical specifications, precision, and measurement uncertainties of the experimental instrumentation

Instrument	Measured Quantity	Accuracy/Resolution	Unit
Stopwatch	Time, Δt	±1	s
Thermocouple (K-type)	Exhaust gas temperature, EGT	±1.5	°C
Tachometer	Engine speed, N	±(0.05% of reading + 1 digit); resolution 1 rpm	rpm
Fuel burette	Fuel volume, ΔVf	±1	mL
Digital voltmeter	Voltage, V	±1% of reading	V
Digital ammeter	Current, I	±1% of reading	A
Fuel density (from reference/measurement)	Fuel density, ρf	±0.5	kg/m³
Calorific value measurement	C.V	±0.1% of reading	kJ/kg

3.3.3 Propagated uncertainty of derived parameters

The uncertainties associated with the derived parameters were evaluated using the RSS method [33, 34].

Fuel mass flow rate uncertainty. The fuel mass flow rate was determined from the measured fuel volume, fuel density, and consumption time:

$$\left(\frac{U_{m \cdot f}}{m \cdot f}\right) = \sqrt{(\frac{U_\rho}{\rho})^2 + (\frac{U_V}{V})^2 + (\frac{U_t}{t})^2} \quad (16)$$

where, $U_{m \cdot f}$ indicate uncertainty in the fuel mass flow rate, U_ρ indicate the uncertainty in fuel density, U_V denotes uncertainty in fuel volume measurement, and U_t denotes the uncertainty in time measurement.

Electrical power output uncertainty. The useful electrical power output was determined from the measured voltage and current of the coupled synchronous generator. The corresponding relative uncertainty was calculated as:

$$\left(\frac{U_{Pelec}}{P_{elec}}\right) = \sqrt{(\frac{U_V}{V})^2+(\frac{U_I}{I})^2} \quad (17)$$

where, $U_{P_{elec}}$ is the uncertainty in the electrical power output, U_V indicate uncertainty in voltage measurement, U_I indicate uncertainty in the current measurement.

Brake Specific Fuel Consumption uncertainty. Since BSFC depends on fuel mass flow rate and electrical power output. Its propagated uncertainty is given by:

$$\left(\frac{U_{BSFC}}{BSFC}\right) = \sqrt{(\frac{U_{m \cdot f}}{m \cdot f})^2+(\frac{U_{P elec}}{P_{elec}})^2} \quad (18)$$

where, U_{BSFC} indicate uncertainty in BSFC, $U_{m \cdot f}$ indicate uncertainty in the fuel mass flow rate, and $U_{P_{elec}}$ indicate uncertainty in the measured electrical power output.

Brake Thermal Efficiency (η_{th}) uncertainty. The uncertainty in η_{th} brake thermal efficiency (BTE) depends on the measured electrical power output, fuel mass flow rate, and lower heating value, $m \cdot_f$ and fuel heating value. The relative uncertainty is expressed as:

$$\left(\frac{U_{BTE}}{BTE}\right) = \sqrt{(\frac{U_{P elec}}{P_{elec}})^2+(\frac{U_{m \cdot f}}{m \cdot f})^2 + (\frac{U_{LHV}}{LHV})^2} \quad (19)$$

where, U_{BTE} indicate uncertainty in BTE, $U_{m \cdot f}$ indicate uncertainty of fuel mass flow rate, $U_{P_{elec}}$ indicate uncertainty in the measured electrical power output, and U_{LHV} indicate uncertainty of the lower heating value.

Exergy Efficiency (η_{ex}) Uncertainty. The uncertainty associated with η_{ex} was calculated from the useful electrical exergy output and the fuel exergy input. Therefore, its propagated uncertainty was evaluated using the same RSS formulation, accounting for uncertainties in the fuel mass flow rate, heating value, and measured thermodynamic quantities.

$$\left(\frac{U_{\eta_{ex}}}{\eta_{ex}}\right) = \sqrt{\left(\frac{U_{P_{elec}}}{P_{elec}}\right)^2 + \left(\frac{U_{\dot{m}_f}}{\dot{m}_f}\right)^2 + \left(\frac{U_{\varepsilon_f}}{\varepsilon_f}\right)^2} \quad (20)$$

The term ε_f denotes the specific fuel exergy, and U_{ε_f} is its associated uncertainty. The calculated propagated uncertainties of the derived parameters are presented in Tables 6-10.

Table 6. Relative uncertainty of fuel mass flow rate

Load (%)	D100	B10	B20	B30	B40	B50
25	2.07	2.08	2.08	2.09	2.09	2.09
50	2.12	2.13	2.14	2.14	2.15	2.16
75	2.19	2.19	2.20	2.22	2.22	2.24
100	2.29	2.31	2.31	2.35	2.37	2.39

Table 7. Relative uncertainty of brake specific fuel consumption (BSFC)

Load (%)	D100	B10	B20	B30	B40	B50
25	2.51	2.51	2.52	2.52	2.52	2.52
50	2.55	2.56	2.56	2.57	2.57	2.58
75	2.61	2.61	2.61	2.63	2.64	2.65
100	2.69	2.71	2.71	2.74	2.76	2.78

Table 8. Relative uncertainty of brake thermal efficiency (BTE)

Load (%)	D100	B10	B20	B30	B40	B50
25	2.51	2.51	2.52	2.52	2.52	2.53
50	2.55	2.56	2.56	2.57	2.58	2.58
75	2.61	2.61	2.62	2.63	2.64	2.65
100	2.69	2.71	2.71	2.75	2.76	2.78

Table 9. Relative uncertainty of fuel exergy rate

Load (%)	D100	B10	B20	B30	B40	B50
25	2.07	2.08	2.09	2.09	2.09	2.09
50	2.13	2.13	2.14	2.15	2.15	2.16
75	2.19	2.19	2.20	2.22	2.23	2.24
100	2.29	2.31	2.32	2.35	2.37	2.40

Table 10. Relative uncertainty of exergy efficiency (η_{ex})

Load (%)	D100	B10	B20	B30	B40	B50
25	2.51	2.51	2.52	2.52	2.52	2.53
50	2.55	2.56	2.56	2.57	2.58	2.58
75	2.61	2.61	2.62	2.63	2.64	2.65
100	2.69	2.71	2.71	2.75	2.76	2.78

The propagated uncertainties of BSFC, BTE, and η_{ex} are relatively similar because these parameters are derived from the same primary measured variables, namely fuel mass flow rate, voltage, current, and fuel calorific value. Among these variables, the uncertainty associated with fuel mass flow rate represents the dominant contribution to the overall propagated uncertainty, whereas the contributions of voltage, current, and fuel calorific value measurements are comparatively smaller. Consequently, the overall propagated uncertainties remained below 3%, indicating acceptable experimental reliability and measurement consistency.

4. RESULTS AND DISCUSSION

4.1 Exergy analysis results

4.1.1 Exergy efficiency

Figure 6 depicts the variation in η_{ex} when an engine operates on a biodiesel blend sourced from WCO under various loads. The results show that η_{ex} progressively increases with increasing load across all utilised fuel types. This behavior may be associated with improved utilisation of fuel exergy and reduced relative thermodynamic losses at higher engine loads. Exergy losses are notably substantial when functioning at a low load of 25%. This behavior may be associated with higher relative heat-transfer losses and increased thermodynamic irreversibility at low-load operation. Consequently, η_{ex} is comparatively low. As the engine load increases toward full-load operation, η_{ex} reaches its highest value. Pure diesel (D100) had the highest η_{ex} and lowest exergy destruction, while medium blends of biodiesel (B10–B20) had a relatively small η_{ex} penalty over diesel. On the other hand, fuel consumption increased, and thermodynamic irreversibility increased with higher biodiesel blends (B30–B50), which led to a progressive decrease in η_{ex} and an increase in exergy destruction.

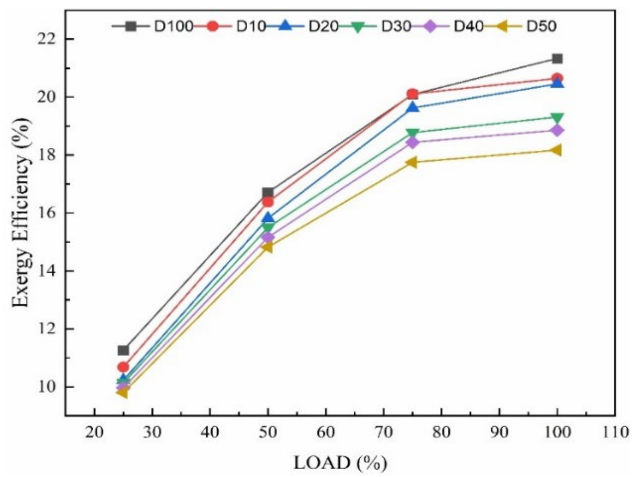

Figure 6. Variation of exergy efficiency (η_{ex}) with engine load

4.1.2 Exergy destruction analysis

The variation of available energy loss rate (exergy destruction rate, $\dot{E}x_{dest}$) of the diesel and biodiesel blends obtained from WCO with respect to the engine loading is illustrated in Figure 7. For all the tested fuel samples, $\dot{E}x_{dest}$ is generally found to rise with the engine load. The increasing trend shows that the internal irreversibility is still the main source of thermodynamic losses on the engine's efficiency. A large part of the chemical energy of the fuel is not available under full load conditions. This increase could be related to thermodynamic irreversibilities and heat transfer losses in the engine system. An increase in the load also increases the exergy-destruction rates and the fuel-exergy input. The increase in loads also results in better engine performance; overall, it is generally related to an increase in thermodynamic irreversibility and an increase in entropy generation as reported in previous studies. In the previous study, the oxygenated content of WCO biodiesel has been reported to be more complete, but it was not directly tested in the current study.

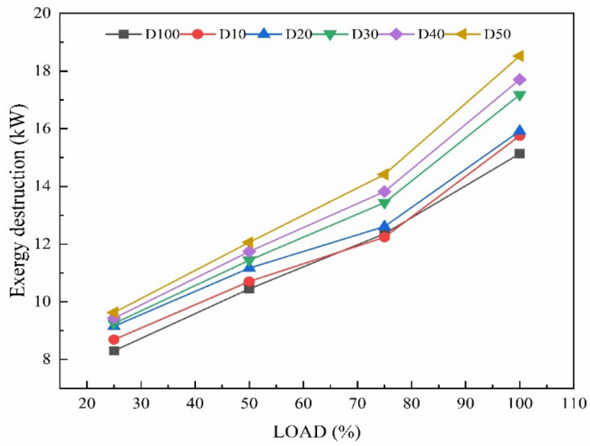

Figure 7. Variation of exergy destruction at different loads

4.1.3 Exergy distribution at full load

A maximum-load distribution of available fuel energy at maximum load is displayed in Figure 8, showing the distribution for different exergy components. It shows that the internal irreversibility of the fuel energy is the major source of loss of energy during full load operation. In the meantime, a lower percentage of energy is lost in the exhaust gases. At full load, the exergy of the exhaust gases increased in importance as a result of the higher T_{exh}, which could make waste-heat recovery applications possible in the future.

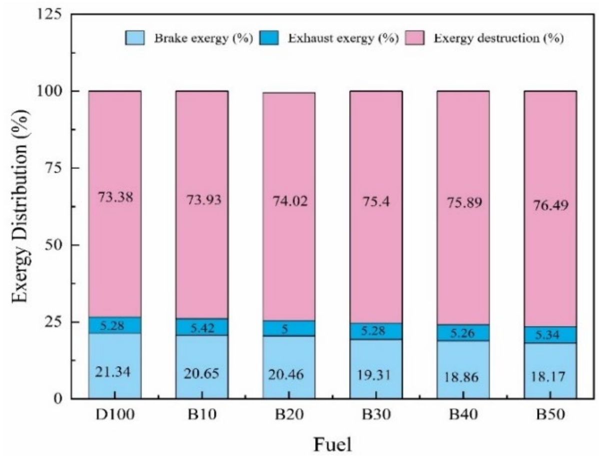

Figure 8. Exergy distribution at full load for diesel and biodiesel blends

4.1.4 Comparative exergy assessment

Table 11 summarises the exergy performance of diesel fuel and WCO biodiesel blends at maximum engine load. D100 exhibited the highest η_{ex} and the lowest absolute exergy destruction rate among all tested fuels. With the increase in blending ratio of biodiesel, the absolute exergy destruction rate (kW) and the exergy destruction percentage increased, and the η_{ex} gradually decreased. It is important to note that the rise in absolute exergy destruction must be taken in conjunction with the rise in fuel exergy consumption and not as a stand-alone measure of poorer thermodynamic performance. In the recent exergy analysis of a diesel engine, similar observations have been reported in which the $\dot{E}x_{dest}$ and η_{ex} have been correlated and interpreted together so as to give a balanced view of the thermodynamics [28]. Medium biodiesel blends (B10–B20) recorded only a slight decrease in the η_{ex} and a little increase in exergy destruction percentage with respect to pure diesel fuel, while the higher biodiesel blends (B30–B50) recorded higher exergy loss as the biodiesel percentage increased. These findings show that as the concentration of biodiesel increases, the utilization factor of fuel exergy will be gradually decreased under full load operating conditions.

Table 11. Summary of exergy parameters and destruction rates at maximum engine load

Fuel	η_{ex} (%)	$\dot{E}x_{dest}$ (kW)	$\dot{E}x_{dest}$ (%)	$\dot{E}x_{exh}$ (%)
D100	21.338	15.132	73.38	5.28
B10	20.646	15.755	73.93	5.42
B20	20.456	15.921	74.02	5.53
B30	19.312	17.18	75.4	5.28
B40	18.86	17.704	75.89	5.26
B50	18.17	18.522	76.49	5.34

4.2 Impact of waste cooking oil biodiesel blends on engine performance

4.2.1 Exhaust Gas Temperature behavior

Figure 9 illustrates the change in exhaust temperature with varying engine loads. The use of pure diesel fuel (D100) and the five biodiesel blends (B10-B50) clearly demonstrate an increase in T_{exh} for all fuel types as the load increases. This behavior may be associated with the higher fuel supply required at increased engine loads, which is generally associated with elevated in-cylinder temperatures, as reported in previous studies. The exhaust temperature when using biodiesel was approximately 6.8% higher than when using pure diesel, especially under full loads. Similar trends have also been reported for WCO biodiesel blends, where the oxygenated nature of biodiesel may influence combustion behavior and EGT under increasing engine loads [34].

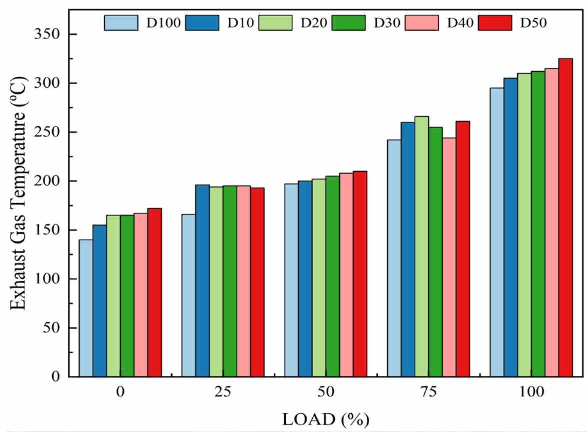

Figure 9. Comparison of exhaust gas temperatures (EGT) of diesel - waste cooking oil (WCO) biodiesel blends at different loads

4.2.2 Engine power characteristics

Figure 10 demonstrates that engine power is influenced by fuel type and is directly proportional to engine load. This behavior may be attributed to the increased energy demand required to satisfy higher engine loading conditions, as reported in previous studies [34]. The results of the tests showed that the electrical power input to the engine–generator system was about 4.9% greater to reach the tested loading conditions, especially for full load. The observed behavior could also be due to the LCV of biodiesel as compared to conventional diesel, which typically needs a higher $\dot{m}_f$ to produce an equivalent electrical power output [35]. A further consideration is the relatively greater density of the biodiesel that could lead to increased fuel delivery per injection as observed in previous studies [35].

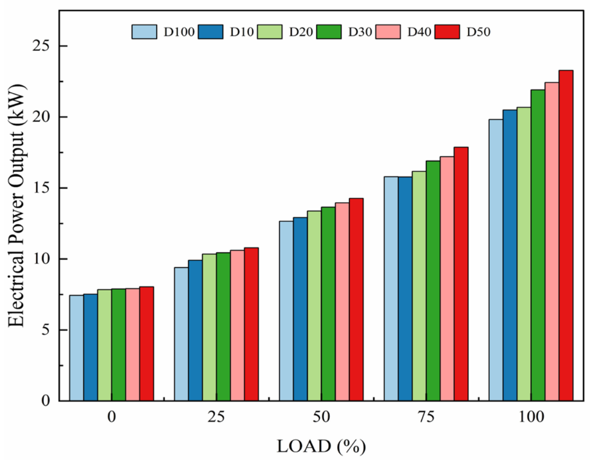

Figure 10. Comparison of electrical power output of diesel - waste cooking oil (WCO) biodiesel blends at different loads

4.2.3 Brake Specific Fuel Consumption behavior

The BSFC results for the engine were documented using various fuel types and loads, as illustrated in Figure 11. At full engine loads, both pure diesel and biodiesel blends showed a lower BSFC value. This trend could correspond with higher fuel-energy efficiencies at higher loads as found in earlier studies [36]. The blends of biodiesel used over-consumed fuel by about 10.7%, primarily due to the LHV of the blends, which meant that the same power output could not be obtained with the same $\dot{m}_f$. In addition, the slightly higher viscosity of biodiesel could affect fuel spray performance and fuel-to-mixture mixing due to the fact that this has been suggested in previous studies [37]. Despite the increase in BSFC, the tested biodiesel blends remained operationally suitable for use in the unmodified diesel engine under the investigated operating conditions.

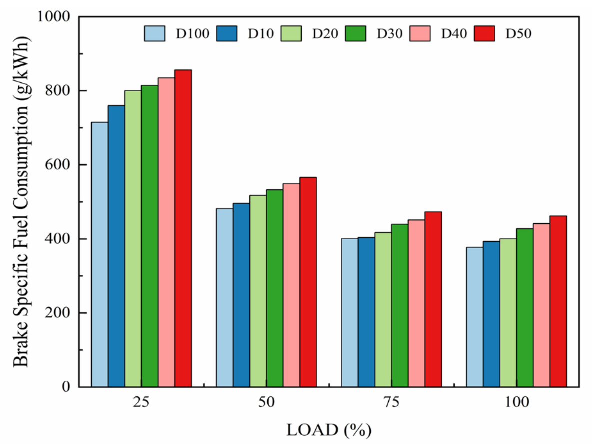

Figure 11. Comparison of brake specific fuel consumption (BSFC) of diesel - waste cooking oil (WCO) biodiesel blends at different loads

4.2.4 Air-Fuel Ratio behavior

Figure 12 illustrates that both fuel type and elevated load substantially affect the air-fuel ratio (AFR). As the load increases, this ratio typically decreases because a greater fuel injection rate is required to maintain constant torque. This leads to a greater fuel mass than the relatively constant intake air mass under stable operating conditions. Under elevated loads, the AFR was approximately 8.3% lower with biodiesel than with diesel fuel. Moreover, the oxygenated nature of biodiesel fuels may influence combustion characteristics under fuel-rich operating conditions, as suggested in previous studies [35]. This behavior has been associated with lower concentrations of incomplete-combustion products in biodiesel-fuelled diesel engines; however, such emissions were not measured in the present study [13].

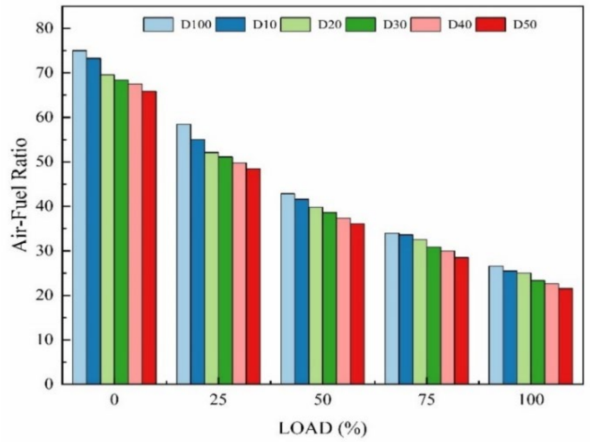

Figure 12. Comparison of air-fuel ratio (AFR) of diesel - waste cooking oil (WCO) biodiesel blends at different loads

4.2.5 Brake Thermal Efficiency behavior

BTE varies with the fuel used and engine load, as shown in Figure 13. BTE increased with increasing engine load for both pure diesel and biodiesel blends. This behavior may be associated with improved utilization of the fuel energy input at higher engine loads and a reduced relative significance of heat losses, as reported in previous studies [36]. The biodiesel blends exhibited approximately 3.6% higher BTE than pure diesel under certain operating conditions. This behavior may be associated with the oxygenated nature of biodiesel fuels, which has been reported to influence combustion characteristics in diesel engines [38]. Conversely, at full loads, the BTE of biodiesel is lower than that of pure diesel. This behavior may be associated with the LHV and relatively higher viscosity of biodiesel fuels, which can influence fuel preparation and combustion processes, as suggested in previous investigations [37]. The results indicate that low- and medium-biodiesel blends can be utilised in the unmodified diesel engine while maintaining acceptable thermal performance under the investigated operating conditions.

4.2.6 Volumetric efficiency behavior

Figure 14 illustrates the variation of volumetric efficiency (VE) in a diesel-biodiesel blend with respect to load. Volumetric efficiency decreased with increasing load for all tested fuels. This behavior may be associated with the higher thermal conditions developed at elevated engine loads, which can influence the density of the inducted air charge, as reported in previous studies [36]. Compared with diesel fuel, the η_v of the biodiesel blend decreased by approximately 3.1% under high-load conditions. This reduction may also be associated with the higher exhaust-gas temperatures observed for biodiesel blends, which may affect the intake process under high-load operating conditions, as suggested in previous investigations [38]. The results indicate that WCO biodiesel blends can be utilised in conventional diesel engines while maintaining acceptable volumetric-efficiency characteristics under the investigated operating conditions.

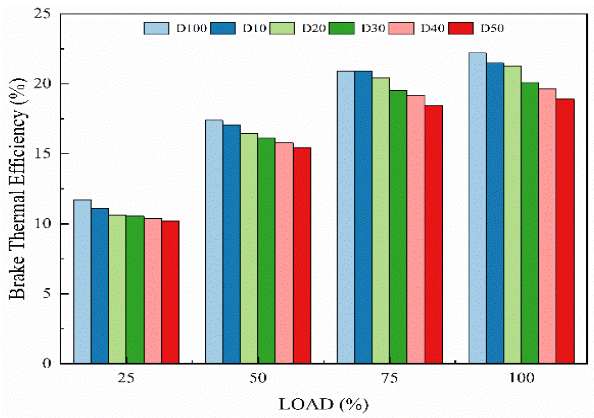

Figure 13. Comparison of brake thermal efficiency (BTE) of diesel - waste cooking oil (WCO) biodiesel blends at different loads

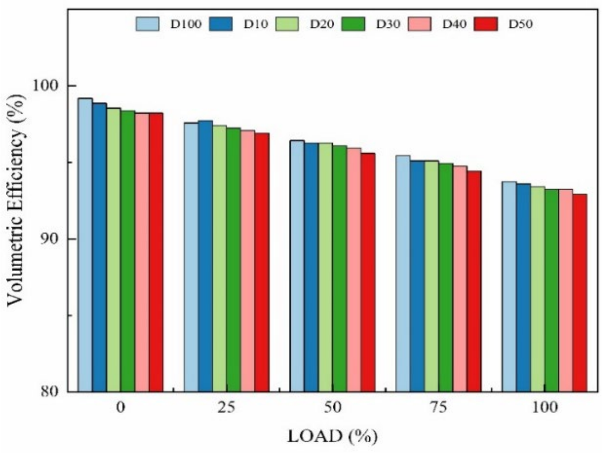

Figure 14. Comparison of volumetric efficiency (VE) of diesel - waste cooking oil (WCO) biodiesel blends at different loads

5. LIMITATIONS OF THE PRESENT STUDY

The present investigation was conducted using a single-cylinder, naturally aspirated diesel engine operating at a constant speed under steady-state conditions. Hence, the results obtained might vary in transient operation or for multi-cylinder engines. Further, there was no in-cylinder pressure analysis carried out, nor a detailed combustion analysis included in the present study, which restricts detailed combustion interpretation. The study also did not include an examination of the long-term durability of the engine, injector deposits or the effects of lubrication during the use of biodiesel for a long period of time. Moreover, the physical exergy of exhaust gases is only taken into account in the exergy analysis; the chemical exergy of the exhaust species is not incorporated in the present analysis. Future investigations may include advanced combustion analysis, transient engine operation, waste heat recovery integration, and long-term durability assessment to provide a more comprehensive thermodynamic evaluation of biodiesel-fuelled diesel engines.

6. CONCLUSION

An experimental thermodynamic and exergy assessment of WCO biodiesel blends was conducted using an unmodified single-cylinder diesel engine under different operating loads. The investigation employed first-law analysis, second-law analysis, and uncertainty propagation to evaluate the thermodynamic performance of biodiesel blends (B10–B50). The results indicated that increasing engine load increased η_{ex} and improved overall thermodynamic performance. The EGT increased by approximately 6.8% for biodiesel blends relative to diesel fuel under high-load conditions, which may be associated with the oxygenated nature and fuel properties of biodiesel blends. The BSFC increased by nearly 10.7% with increasing biodiesel concentration owing to the LCV and higher viscosity of biodiesel blends. Meanwhile, the AFR and volumetric efficiency decreased by approximately 8.3% and 3.1%, respectively, under full-load operation.

Exergy analysis revealed that η_{ex} improved with increasing load and reached a maximum value of 21.34% for D100 at full load. In contrast, exergy destruction increased progressively with increasing biodiesel concentration, rising from 15.13 kW for D100 to 18.52 kW for B50. The exergy distribution analysis further indicated that the major portion of fuel exergy was associated with exergy destruction within the adopted exergy-based thermodynamic assessment, whereas exhaust exergy remained within the range of 5.26–5.53%, suggesting potential opportunities for future waste heat recovery applications.

The uncertainty analysis confirmed acceptable reliability of the experimental measurements and calculated parameters, with propagated uncertainty values remaining within approximately 2–3%. Overall, the study demonstrates that low- and medium-WCO biodiesel blends (B10–B20) can be applied in conventional diesel engines under practical operating conditions with only a modest thermodynamic performance penalty compared with pure diesel. In contrast, higher biodiesel blends (B30–B50) exhibited progressively lower η_{ex} and higher exergy destruction. Therefore, low- and medium-biodiesel blends represent a practical compromise between thermodynamic performance and reduced dependence on conventional petroleum diesel fuel.

REFERENCES

[1] Al-Jabiri, A.A., Balla, H.H., Al-Zuhairy, M.S. (2024). Using renewable alternative fuels and studying their impact on the performance and emissions of compression ignition engines. Heat Transfer, 53(4): 1975-1988. https://doi.org/10.1002/htj.23029
[2] Ali, N., Maki, D.F. (2023). Combustion characteristics of CI engine fueled with WCO biodiesel/diesel blends at different compression ratios and EGR. Heat Transfer, 52(6): 3953-3966. https://doi.org/10.1002/htj.22859
[3] Al-Kaabi, M.M., Balla, H.H., Al-Zuhairy, M.S. (2020). Performance study of single cylinder engine dual fuel (diesel + LPG). IOP Conference Series: Materials

Science and Engineering, 928: 022098. https://doi.org/10.1088/1757-899X/928/2/022098

[4] Kumar, N., Varun, Chauhan, S.R. (2013). Performance and emission characteristics of biodiesel from different origins: A review. Renewable and Sustainable Energy Reviews, 21: 633-658. https://doi.org/10.1016/j.rser.2013.01.006

[5] Buyukkaya, E. (2010). Effects of biodiesel on a DI diesel engine performance, emission and combustion characteristics. Fuel, 89(10): 3099-3105. https://doi.org/10.1016/j.fuel.2010.05.034

[6] Venu, H., Raju, V.D., Nair, J.N., et al. (2025). Exergy and energy-based sustainability evaluation of diesel-biodiesel-ethanol blends with emission forecasting using advanced machine learning models. Case Studies in Thermal Engineering, 73: 106516. https://doi.org/10.1016/j.csite.2025.106516

[7] Doppalapudi, A.T., Azad, A.K., Ahmed, S.F. (2026). Experimental exergy and energy analysis of Ungurahui biodiesel blended with ethers to reduce emissions. Energy Conversion and Management: X, 30: 101788. https://doi.org/10.1016/j.ecmx.2026.101788

[8] Hossain, F.M., Nabi, M.N., Rainey, T.J., et al. (2017). Investigation of microalgae HTL fuel effects on diesel engine performance and exhaust emissions using surrogate fuels. Energy Conversion and Management, 152: 186-200. https://doi.org/10.1016/j.enconman.2017.09.016

[9] Schaeffer, R., Erickson, P., Guivarch, C., Brutschin, E., Pye, S. (2023). Global fossil fuel reduction pathways under different climate mitigation strategies and ambitions. Nature Communications, 14. https://doi.org/10.1038/s41467-023-41105-z

[10] Singh, D., Sharma, A.K., Patanwar, P., Jangde, P.K. (2025). Exergy, energy and emissions analyses of biodiesel-diesel blends in a diesel engine. Transactions on Energy Systems Engineering and Applications, 6(2): 1-18. https://doi.org/10.32397/tesea.vol6.n2.709

[11] Sulochana, G., Bhatti, S.K. (2019). Performance, emission and combustion characteristics of a twin cylinder 4 stroke diesel engine using nano-tubes blended waste fry oil methyl ester. Materials Today: Proceedings, 18: 75-84. https://doi.org/10.1016/j.matpr.2019.06.279

[12] Mohammad, A.S., Balla, H.H., Al-Zuhairy, M.S. (2023). Emission and performance in a diesel engine operating on diesel-biodiesel-butanol blends derived from waste cooking oil. International Journal of Energy Production and Management, 8(4): 241-249. https://doi.org/10.18280/ijepm.080406

[13] Meng, J., Xu, W., Meng, F., et al. (2023). Effects of waste cooking oil biodiesel addition on combustion, regulated and unregulated emission characteristics of common-rail diesel engine. Process Safety and Environmental Protection, 178: 1094-1106. https://doi.org/10.1016/j.psep.2023.08.065

[14] Rajendran, S. (2021). A comparative study of performance and emission characteristics of neat biodiesel operated diesel engine: A review. Journal of Thermal Analysis and Calorimetry, 146(3): 1015-1025. https://doi.org/10.1007/s10973-020-10121-2

[15] Özener, O., Yüksek, L., Ergenç, A.T., Özkan, M. (2014). Effects of soybean biodiesel on a DI diesel engine performance, emission and combustion characteristics. Fuel, 115: 875-883. https://doi.org/10.1016/j.fuel.2012.10.081

[16] Abed, K.A., El Morsi, A.K., Sayed, M.M., El Shaib, A.A., Gad, M.S. (2018). Effect of waste cooking-oil biodiesel on performance and exhaust emissions of a diesel engine. Egyptian Journal of Petroleum, 27(4): 985-989. https://doi.org/10.1016/j.ejpe.2018.02.008

[17] Sayyed, S., Das, R.K., Kulkarni, K. (2022). Experimental investigation for evaluating the performance and emission characteristics of DICI engine fueled with dual biodiesel-diesel blends of Jatropha, Karanja, Mahua, and Neem. Energy, 238: 121787. https://doi.org/10.1016/j.energy.2021.121787

[18] Mathew, A., Anand, K. (2021). Comparison of engine characteristics with biodiesels produced from fresh and waste cooking oils. Biofuels, 12(6): 663-671. https://doi.org/10.1080/17597269.2018.1519761

[19] Ghaffarzadeh, S., Marami Milani, S. (2025). Energy and exergy analysis of low-temperature combustion in a light-duty diesel/CNG and biodiesel/CNG fueled engine. Energy Conversion and Management: X, 28: 101371. https://doi.org/10.1016/j.ecmx.2025.101371

[20] Hasan, K.S., Balla, H.H. (2026). A review of variable compression ratio diesel engines: Performance, emissions, and renewable fuels. Journal of Science and Engineering Applications, 8(1). https://doi.org/10.66262/1vtz5h28

[21] Abedin, M.J., Masjuki, H.H., Kalam, M.A., Sanjid, A., Ashraful, A.M. (2014). Combustion, performance, and emission characteristics of low heat rejection engine operating on various biodiesels and vegetable oils. Energy Conversion and Management, 85: 173-189. https://doi.org/10.1016/j.enconman.2014.05.065

[22] Datta, A., Mandal, B.K. (2016). A comprehensive review of biodiesel as an alternative fuel for compression ignition engine. Renewable and Sustainable Energy Reviews, 57: 799-821. https://doi.org/10.1016/j.rser.2015.12.170

[23] Kolhe, N.S., Gupta, A.R., Rathod, V.K. (2017). Production and purification of biodiesel produced from used frying oil using hydrodynamic cavitation. Resource-Efficient Technologies, 3(2): 198-203. https://doi.org/10.1016/j.reffit.2017.04.008

[24] Baluchamy, A., Saravanamuthu, M., Natarajan, S.S., Chandramurthy, S.R. (2025). Analysis of energy, exergy, and emissions in a diesel engine powered by cotton silk seed oil biodiesel with varying injection timings. Environmental Science and Pollution Research, 32: 31703-31717. https://doi.org/10.1007/s11356-025-35957-9

[25] Pullagura, G., Bikkavolu, J.R., Prasad, V.V.S., Prathipati, R., Seepana, P. (2025). Energy, exergy, and sustainability assessments of a compression ignition diesel engine fueled with Pongamia pinnata oil-diesel blends and nanoparticles. Emergent Materials, 8(1): 199-215. https://doi.org/10.1007/s42247-024-00962-0

[26] Wang, Y., Sedghi, R., Shahbeik, H., et al. (2024). A comprehensive review of exergy analysis in biodiesel-powered engines for sustainable power generation. Sustainable Energy Technologies and Assessments, 68: 103869. https://doi.org/10.1016/j.seta.2024.103869

[27] Doğan, B., Erol, D. (2023). The investigation of energy and exergy analyses in compression ignition engines using diesel/biodiesel fuel blends: A review. Journal of Thermal Analysis and Calorimetry, 148(5): 1765-1782.

https://doi.org/10.1007/s10973-022-11862-y

[28] Raouf, E.A., Sadig, H. (2026). Predictive exergy-based framework for assessing diesel engine performance under variable load conditions using Diesel-RK. International Journal of Heat and Technology, 44(2): 803-813. https://doi.org/10.18280/ijht.440230

[29] Degfie, T.A., Mamo, T.T., Mekonnen, Y.S. (2019). Optimized biodiesel production from waste cooking oil (WCO) using calcium oxide (CaO) nano-catalyst. Scientific Reports, 9(1). https://doi.org/10.1038/s41598-019-55403-4

[30] Camilo, G.L., Queiroz, A., Ribeiro, A.E., Gomes, M.C.S., Brito, P. (2024). Review of biodiesel production using various feedstocks and its purification through several methodologies, with a specific emphasis on dry washing. Journal of Industrial and Engineering Chemistry, 136: 1-15. https://doi.org/10.1016/j.jiec.2024.02.016

[31] Prasetiyo, D.H.T., Sanata, A., Sidartawan, R., Trifiananto, M., Abidin, A., Supraptiningsih, L. (2025). Study of viscosity and density changes of waste cooking oil biodiesel due to gradual heat treatment. Energy: Jurnal Ilmiah Ilmu-Ilmu Teknik, 15(1): 1-12. https://doi.org/10.51747/energy.v15i1.1511

[32] Adhikesavan, C., Ganesh, D., Augustin, V.C. (2022). Effect of quality of waste cooking oil on the properties of biodiesel, engine performance and emissions. Clean Chemical Engineering, 4: 100070. https://doi.org/10.1016/j.clce.2022.100070

[33] Leng, L., Yang, X., Shi, L., Deng, K. (2026). Experimental investigation of energy coupling mechanism and regulation strategies for turbocompound engine efficiency enhancement. Energy Conversion and Management, 348: 120674. https://doi.org/10.1016/j.enconman.2025.120674

[34] Genet, N., Menelik, M., Mekonen, W., Gzate, Y., Leul, A., Demisie, F. (2024). Experimental investigation on diesel engine performance and emission characteristics using waste cooking oil blended with diesel as biodiesel fuel. Discover Energy. https://doi.org/10.1007/s43937-024-00051-7

[35] Selvam, M., Pragadish, N., Harish, K.A., Srinivasan, R.G., Devarajan, Y., Kaliappan, N. (2025). Investigating emission characteristics and combustion performance of a CRDI engine utilizing novel biodiesel derived from waste cooking oil and pentanol blends. Scientific Reports, 15: 14742. https://doi.org/10.1038/s41598-025-98462-6

[36] Erol, D., Gülcan, H.E. (2025). Energy, exergy, greenhouse gas emission impact and economic analysis of a water-cooled diesel engine running on different proportions of waste cooking oil biodiesel. International Journal of Automotive Engineering and Technologies, 14(3): 154-169. https://doi.org/10.18245/ijaet.1705733

[37] Kuti, O.A., Nishida, K. (2025). An investigation into spray combustion processes of waste cooking oil biodiesel fuel under diesel engine conditions using the LIF-PIV, shadowgraph, and chemiluminescence techniques. International Journal of Thermofluids, 26: 101066. https://doi.org/10.1016/j.ijft.2025.101066

[38] Azarudeen, J.M., Anish, M., Babu, L.G., et al. (2025). Performance and emission characteristics of waste cooking oil biodiesel blends in sustainable fuel applications. Scientific Reports, 15: 35184. https://doi.org/10.1038/s41598-025-19130-3

NOMENCLATURE

A_0	Orifice area
AFR	Air-fuel ratio
BSFC	Brake specific fuel consumption, g/kWh
BTE	Brake thermal efficiency, %
VE	Volumetric efficiency
C_p	Specific heat capacity at constant pressure, kJ/kg·K
CV	Calorific value, kJ/kg
I	Current, A
LHV	Lower heating value, kJ/kg
LCV	Lower calorific value, kJ/kg
N	Engine speed, rpm
P_0	Reference pressure (dead state), atm
P_{elec}	Electrical power output, kW
T	Temperature, K
T_0	Reference temperature (dead state), K
T_{exh}	Exhaust gas temperature, K
U_x	Uncertainty of the measured parameter, %
U_y	Uncertainty of the derived parameter, %
V	Voltage, V
Δt	Time interval, s
ΔV_f	Fuel volume consumed, mL
$\dot{E}x_{dest}$	Exergy destruction rate, kW
$\dot{E}x_{pelec}$	Electrical exergy rate, kW
$\dot{E}x_{exh}$	Exhaust exergy rate, kW
$\dot{E}x_{fuel}$	Fuel exergy rate, kW
$\dot{m}_a$	Air mass flow rate, kg/s
$\dot{m}_{exh}$	Exhaust gas mass flow rate, kg/s
$\dot{m}_f$	Fuel mass flow rate, kg/s
X	Chemical exergy factor

Greek symbols

η_{ex}	Exergy efficiency, %
η_V	Volumetric efficiency, %
ρ_f	Fuel density, kg/m³

Subscripts

WCO	Waste cooking oil
D	Diesel
B	Biodiesel
DI	Direct injection
CR	Compression ratio
RPM	Revolutions per minute
EGT	Exhaust gas temperature
CO	Carbon monoxide
CO_2	Carbon dioxide
HC	Hydrocarbon
NO_x	Nitrogen oxides
PM	Particulate matter
RSS	Root-sum-square method
CI	Compression ignition